Experimental Studies on the Elastic-Plastic Behavior of Braced Frames under Repeated Horizontal Loading

Part 2 Experiments of braces composed of steel circular tubes, angle-shapes, flat bars or round bars

By Minoru WAKABAYASHI, Takeshi NAKAMURA and Nozomu YOSHIDA

(Manuscript received October 2, 1979)

Abstract

Experimental studies are conducted to investigate the hysteretic restoring force characteristics of steel braces built in a structural frame and the effect of the local behavior on the failure. Test specimens of the braces are made of steel circular tubes, angle-shapes, flat bars and round bars. The fundamental properties of hysteretic characteristics of braces with various types of cross sections are extracted from the experimental results. The shape of hysteresis loops, the change and the deterioration in load carrying capacity and energy absorbing capacity under cyclic loading are examined and compared with those of the braces with an H-shaped cross section which was reported in Part 1[1]. It is noted that the reduction of ductility in the plastic deformation range due to cracking at the end-joint portions where stress-concentration might occur in the case of circular tube braces and cracks caused by low cycle fatigue at the end section where bolt holes reduce net area of a cross section and at the locally buckled mid-length portion in the case of angle braces are ascertained.

1. Introduction

This paper discusses on the hysteretic restoring force characteristics of steel braces built in a frame under alternately repeated horizontal loading as well as ductility in the plastic deformation range on the basis of the experimental investigation. The objectives of this series of experimental studies are to clarify the hysteretic behaviors of the existing steel braces and bracing systems and to grasp the behavior of braces coming to the failure or the breakage, aiming at the formulation of a hysteretic rule for restoring force characteristics and the establishment of an earthquake-resistant design method of bracing systems. In part 1 of the paper which was published in September 1977,[1] the braces with an H-shaped cross section were treated. In this report, braces made of circular steel tubes, angle-shapes, flat bars and round bars are treated. As the types of a cross section of brace specimens, frequently used ones in the actual design have been selected. In designing details of the specimens, consideration has been paid to realize the condition which would be similar to that of the braces built in actual structures. Welded joints with a gusset plate and bolted joints with a gusset plate and high strength bolts have been selected as widely used types of the end connection of braces. Peculiar characteristics of the circular tube and angle specimens reported in this paper are that their post-buckling behavior and the subsequent behavior might be influenced by local deformation such as distortion of a cross sectional shape or local buckling and that there would be some difficulties in the estimation of the supporting and continuity conditions at the

end and the estimation of the effective length for buckling because the behavior of the end connection would be complicated due to a complexity in design details. In the case of flat bar braces and round bar braces, no load carrying capacity under compression is expected because of an extremely large slenderness ratio. In the case of round bar braces, the effects of pre-tension is also examined.

2. Test Plan

2.1 Planning of tests

This experimental investigation on the hysteretic restoring force characteristics of steel braces put in a framed building structure has been planned covering the following four types of braces.

(i) braces made of steel circular tubes
(ii) braces made of angle-shapes
(iii) braces made of flat bars
(iv) pre-tensioned braces made of steel round bars

These types of braces are peculiar in the following points.

(i) Circular tube braces

There are some difficulties in a reasonable estimation of the supporting and continuity conditions at the ends and the effective length, because of the discontinuity of uniformity of a cross section due to the existence of gusset plates welded in the slits at the tube ends.

(ii) Angle braces

Complicated behavior due to torsional deformation according to buckling or local buckling originated by a small flexural-torsional rigidity or a comparatively large width-thickness ratio in legs is anticipated. Supporting conditions at the ends are complicated due to bolted joints using gusset plates.

(iii) Flat bar braces

They are usually designed considering only the load carrying capacity in tension and neglecting the small load carrying capacity in compression due to the large slenderness ratio.

(iv) Pre-tensioned round bar braces

The slenderness ratio is also large as in the case of flat bar braces, but the braces would be effective in both compression and tension loading, until the pre-tension is lost.

In short, in this paper, the restoring force characteristics of braces such as steel tube braces or angle braces, which are frequently used in an actual design and are difficult to be idealized as a simple analytical model in a theoretical analysis, and the hysteretic behavior of the braces with a large slenderness ratio are investigated experimentally.

2.2 Test Specimens

There are nine test specimens for steel tube braces, ten for angle braces, two for flat bar braces and two for pre-tensioned round bar braces. Half of the specimens are to be tested under a monotonically increased horizontal loading, and the other half is to be tested under cyclicly repeated loading. The process of fabricating and the dimensions of each type of specimen are as follows:

(a) Steel tube brace specimens

Specimens were made of steel circular tubes of grade JIS–STK 41 with 42.7 mm external diameter and 3.5 mm thickness in nominal sizes. A gusset plate with 12 mm thickness is fillet-welded into the slits at the end of a steel tube while the ends of a tube are covered by steel caps with a quarter of a sphere shape. Adequacy in design and proportioning of the end joint is certified in the preliminary tension test of simple elemental specimens. Shapes and dimensions of steel tube brace specimens are shown in **Fig. 1**(**a**) and (**b**). Specimens for the preliminary tension test are shown in **Photo 1** and an example of the results is shown in **Fig. 2**. The elemental specimens show a satisfactory performance in strength and ductility.

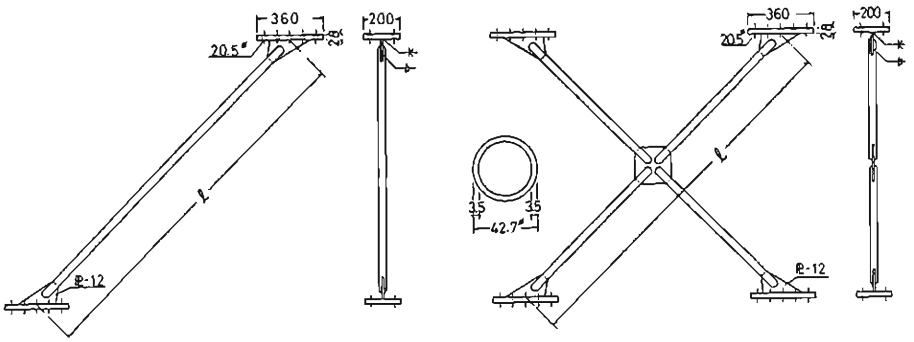

(a) Single Bracing System (b) Double Bracing System

Fig. 1. Steel Tube Brace Specimen.

Photo. 1. Specimens of Preliminary Tension Test of Steel Tube Braces.

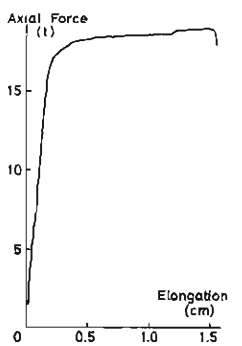

Fig. 2. Examples of Preliminary Tension Test for Steel Tube Brace.

(b) Angle brace specimens

Angle brace specimens except the most stubby X-type double bracing specimens are composed of a pair of L–50×50×4 angle shapes with 50 mm leg length and 4 mm leg thickness of grade JIS–SS41 steel. Two pieces of angles, which are cut to the prescribed length are compounded with a separator plate of 19 mm thickness by 16 mm diameter high strength bolts of grade F10T. Angles are bolted to gusset plates of 19 mm thickness which are butt-welded to the end plate to be fixed rigidly

to a surrounding frame. In the most stubby X-type double bracing specimens (DAC 1, DAM 1), brace elements are made of a single angle. Shapes and dimensions of the specimens are shown in **Figs. 3(a)~(d)**.

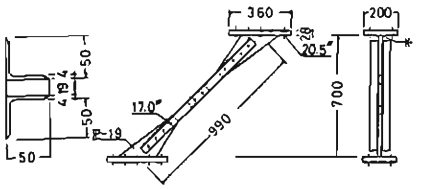

(a) Single Bracing System (l=1 m)

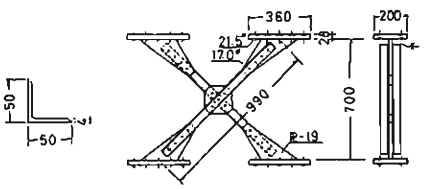

(c) Double Bracing System (l=1 m)

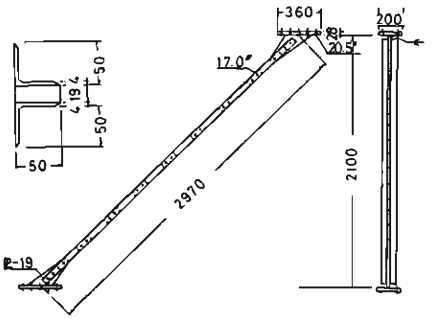

(b) Single Bracing System (l=3 m)

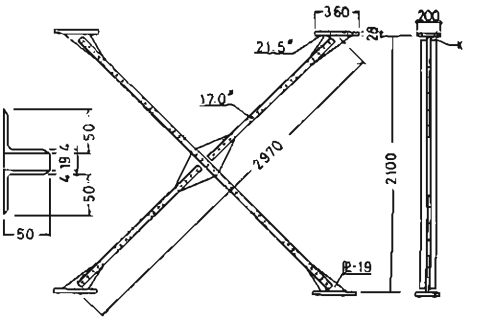

(d) Double Bracing System (l=3 m)

Fig. 3. Angle Brace Specimen.

Preliminary tension tests of the elemental compound members with bolt connections were performed before the main tests, to investigate the fundamental property and strength of bolted section of braces. Test specimens of the preliminary tension tests and an example of the test results are shown in **Photo. 2** and **Fig. 4**, respectively. Bolt jointed parts of elemental specimens show a satisfactory performance.

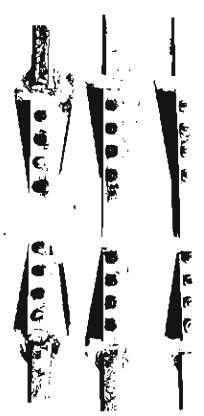

Photo. 2. Specimens of Preliminary Tension Test of Angle Braces.

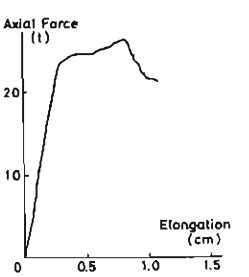

Fig. 4. Examples of Preliminary Tension Test for Angle Brace.

(c) Flat bar brace specimens

Dimensions of one flat bar brace are 35 mm in width, 3.2 mm in thickness and 693 mm in length. The grade of steel is equivalent to JIS–SS50. Both ends of the specimen could be considered to be rigidly supported by a loading frame. The effective slenderness ratio equals 364. **Photo. 3** shows a test specimen and a loading frame.

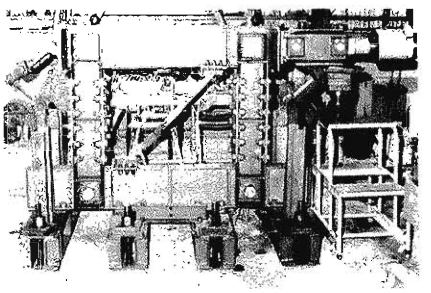

Photo. 3. Test Specimen and Set-up of Flat Bar Braces.

(d) Round bar brace specimens

Specimens are made of commonly used round bars for the reinforcement of reinforced concrete structures. A bar is 16 mm in diameter and SR24 in grade. The bars are welded to a gusset plate of 16 mm thickness, which is connected to the supporting block by a high strength bolt to realize the pinned supporting condition. A turn-buckle is put in the intermediate portion of the bar to introduce pre-tension. **Fig. 5** shows the bar brace specimen.

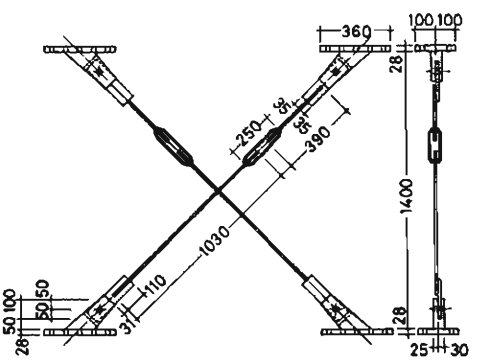

Fig. 5. Round Bar Brace Specimen.

All specimens are tabulated in **Table 1**.

2.3 Test set-up and measurement

Test set-up and system of deformation measurement in the experiments of steel circular tube braces, angle braces and round bar braces are identical with those in the experiments of the braces with an H-shaped cross section which were reported in Part 1.[1] The brace specimen is set in the surrounding frame, which is designed

Table 1. Test Parameters and Dimension of the Specimen

Specimen*1 Name	Type of Brace	Bracing System	Loading*2	B (cm)	t (cm)	l (cm)	l' (cm)	λ_1*3	λ_2*3	λ_3*3
SPM1	Steel Tube	Single Bracing	M	4.30	0.348	98.7	62.7	35.5	71.0	37.7
SPC1			C	4.30	0.347	99.3	63.3	35.5	71.0	37.7
SPM3			M	4.29	0.345	297.0	261.0	106.8	213.5	108.9
SPC3			C	4.29	0.345	296.9	260.9	106.8	213.5	108.9
DPM1		Double Bracing	M	4.30	0.347	98.5	62.5	35.5		
DPC1			C	4.30	0.346	98.3	62.3	35.5		
DPM2			M	4.28	0.349	197.6	161.6	71.1		
DPM3			M	4.30	0.348	296.5	260.5	106.8		
DPC3			C	4.30	0.343	296.8	260.8	106.8		
SAM1	Angle	Single Bracing	M	4.97	0.388	99.8	69.8	20.6	41.2	41.6
SAC1			C	5.01	0.391	99.5	69.5	20.6	41.2	41.6
SAM3			M	4.97	0.377	296.2	266.2	85.3	170.6	106.3
SAC3			C	5.01	0.381	297.2	267.2	85.3	170.6	106.3
DAM1		Double Bracing	M	4.99	0.389	99.3	69.3	33.7		
DAC1			C	4.99	0.389	99.5	69.5	33.7		
DAM2			M	4.99	0.376	198.7	168.7	52.9		
DAC2			C	5.00	0.380	198.3	168.3	52.9		
DAM3			M	5.04	0.389	297.1	267.1	83.3		
DAC3			C	5.00	0.389	296.9	266.9	83.3		
FTBM	Flat Bar	Single Bracing	M	3.53	0.330	69.3	69.3	364	727	
FTBC			C	3.53	0.330	69.3	69.3	364	727	
RB4M	Round Bar	Double Bracing	M	1.58		171.9	101.3		435	
RB4C			C	1.58		171.8	101.2		435	

*1 In the case of steel tube and angle braces, each letter represents test parameters.
S: Single Bracing, D: Double Bracing, P: Steel Tube Brace, A:Angle Brace,
M: Monotonic Loading, C: Cyclic Loading, 1, 2, 3: Length of Brace (unit; m).

*2 M: Monotonic Loading, C: Cyclic Loading

*3 Nominal Dimensions are used for the calculation of slenderness ratio.

not to resist any horizontal load. A general view of the test set-up for the tests of braces except flat bars is shown in **Photo 4**. The set-up of the experiment of the flat bar braces are identical with that in the experiments of reinforced concrete shear walls, in which steel flat bar braces were encased, which was reported in Ref. 2).

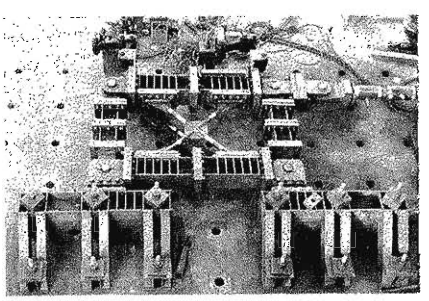

Photo. 4. Whole View of Test.

2.4 Loading Program

The loading in the cyclic tests has been controlled on the basis of the amplitude of the relative horizontal displacement between the upper end and the lower end of a brace except that the first two cycles of loading for the pre-tensioned round bar braces were controlled by load amplitude. The loading programs for circular tube braces and angle braces, flat bar braces and round bar braces are illustrated in **Figs. 6(a)**, **6(b)** and **6(c)**, respectively. Loading was conducted according to these loading programs and terminated when the breakage took place in a brace in tension or a crack expanded so severely that was just about to break.

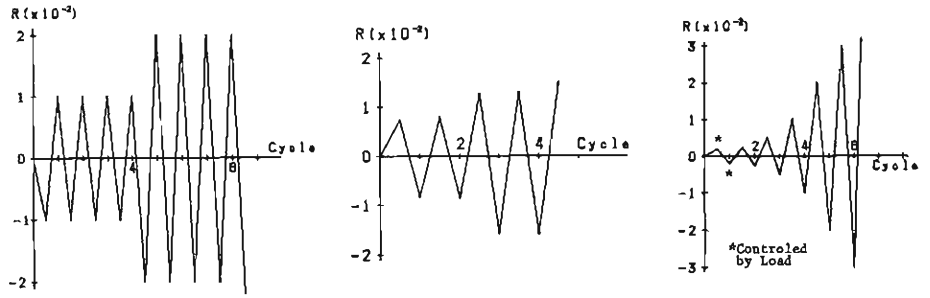

(a) Steel Tube and Angle Braces (b) Flat Bar Braces (c) Round Bar Braces

Fig. 6. Loading Programs.

3. Process and Results of Tests

3.1 Results of coupon tests of materials

The results of tensile tests for materials of the brace specimens are tabulated in **Table 2**. No. 1 type of coupon specimens provided in JIS Z 2201 for angle shapes, No. 12 type coupon specimens for circular tubes and No. 2 type coupon specimens for round bars were tested. In the case of a flat bar specimen, the result of a monotonic tensile test for a brace specimen was substituted. As previously mentioned, preliminary tensile tests for elemental specimens with connections has been performed for circular tubes and angle-shapes before brace specimens were fabricated. The results of these preliminary tests are listed in **Table 2**.

In the data analysis, the results of coupon tests are used.

Table 2. Mechanical Properties of Materials

	Steel Tube	Angle	Flat Bar	Round Bar
Yield Stress (t/cm²)	4.29 (4.4)	3.55	3.0	2.92
Maximum Stress (t/cm²)	5.11 (5.1)	4.98	4.9	4.44
Strain Hardening Strain (%)	2.22	2.57		2.60
Ultimate Strain (%)	20.4		23	28.6
Maximum Stress of Joint Elementary Tension Test (t/cm²)	4.34	3.87		

3.2 Process and results of experiments and behavior of each type of braces

In this section, the peculiar behavior of each type of braces observed in the experiments and the experimental restoring force characteristics are described. In the figures which show restoring force characteristics of braces, those are **Figs. 7**, **8**, **9** and **10**, the ordinate denotes non-dimensionalized restoring force of braces (H/H_y), which was obtained by dividing the observed horizontal load by the horizontal load carrying capacity when the braces were assumed to yield in pure tension and the abscissa denotes non-dimensionalized relative horizontal displacement between the upper and lower ends of braces (Δ/Δ_y) which was obtained by dividing the observed relative displacement by the relative displacement when the braces were assumed

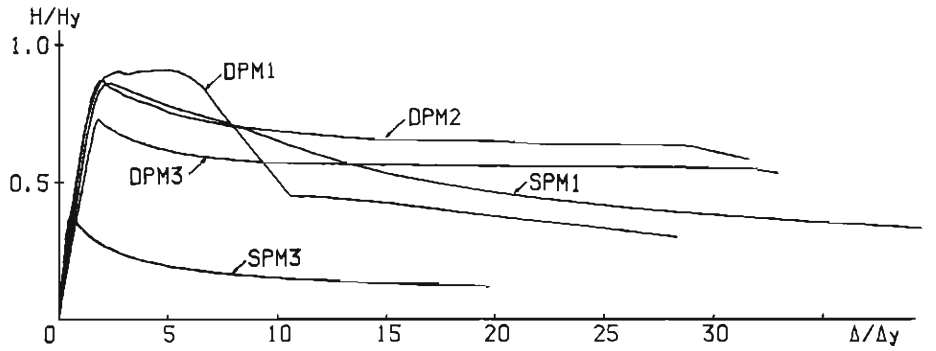

(a) Monotonically Loaded Specimen

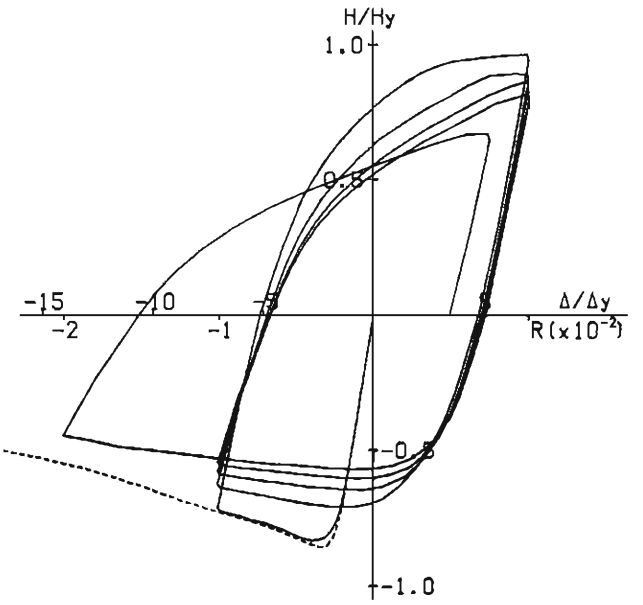

(b) SPC1

Fig. 7. H/H_y–Δ/Δ_y Relation of Steel Tube Braces.

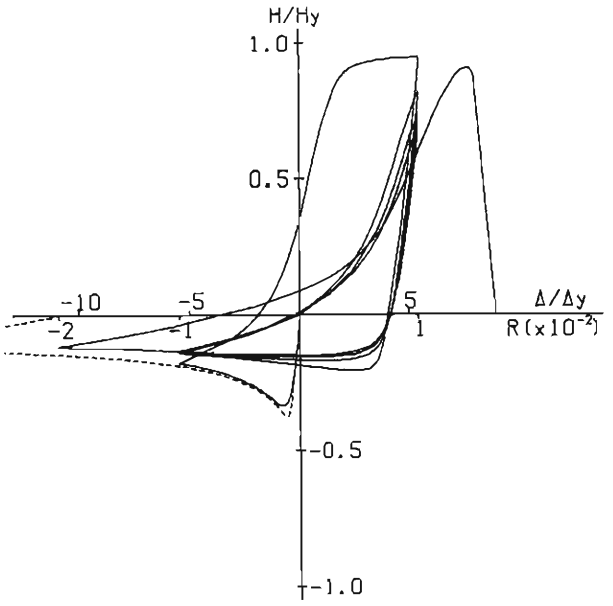

(c) SPC3

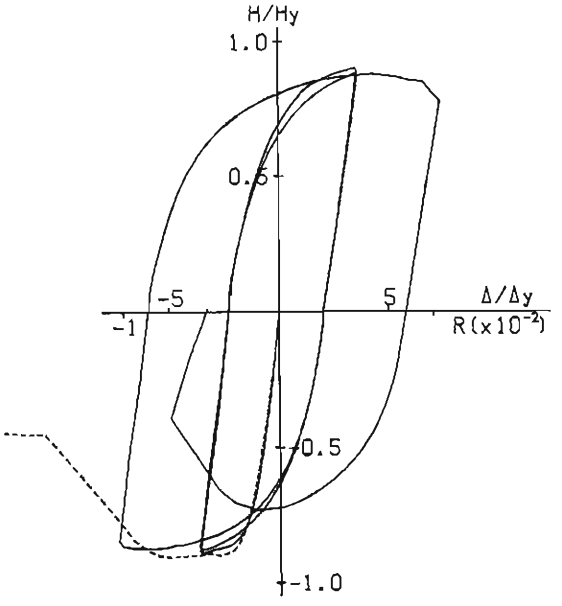

(d) DPC1

Fig. 7. H/H_y-Δ/Δ_y Relation of Steel Tube Braces.

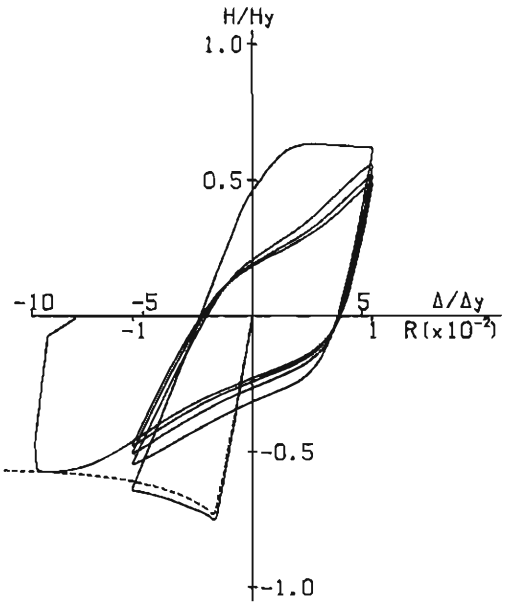

(e) DPC3

Fig. 7. H/H_y–Δ/Δ_y Relation of Steel Tube Braces.

to yield in pure tension. The sub-scale R in the abscissa denotes the story-drift angle, which is obtained by dividing the relative horizontal displacement between the upper and the lower ends of a brace by the clear height of a story. In the case of a single bracing system, first cycle of loading starts in the direction in which the specimen is subjected to compression. Tension and elongation are positive in the figure. In the case of a double bracing system, the first cycle of loading starts on the negative side.

(1) Behavior of circular tube braces

The results of monotonic loading tests of circular tube braces are shown in **Fig. 7(a)**, and those of cyclic loading are shown in **Figs. 7(b)~7(e)**. **Photos. 5(a)** and **5(b)** show the examples of the specimens after testing.

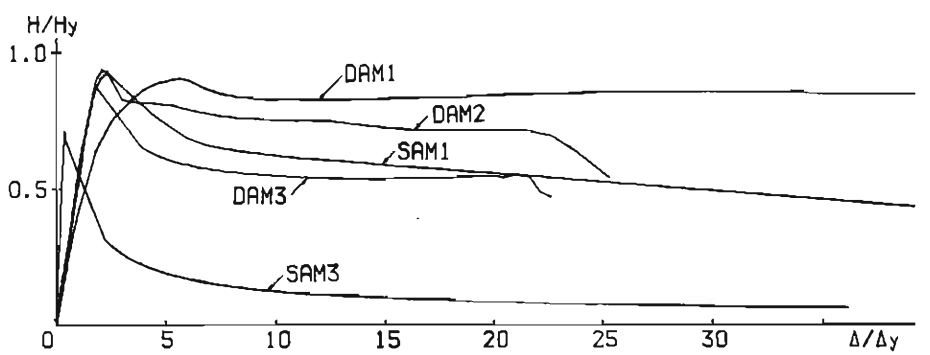

(a) Monotonically Loaded Specimen

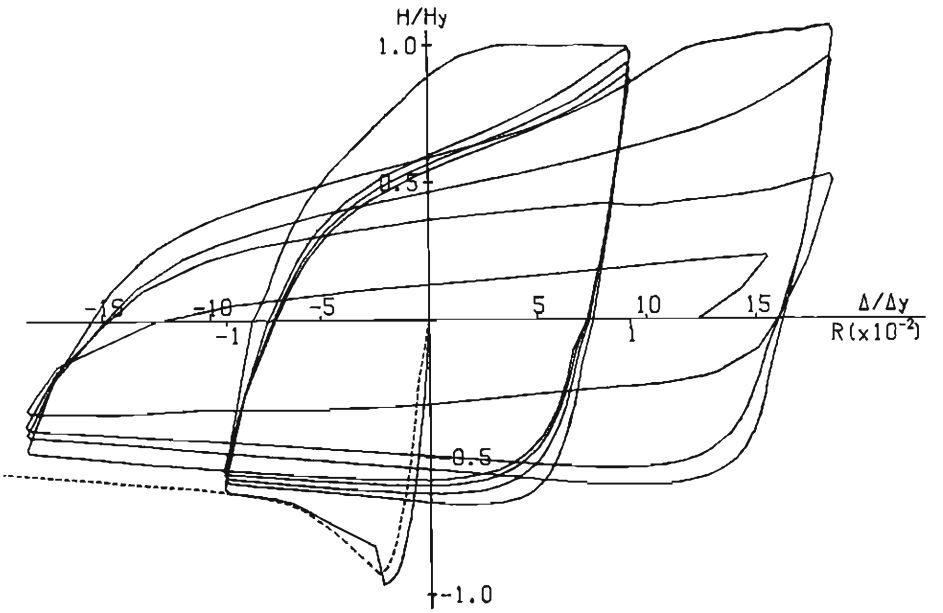

(b) SAC1

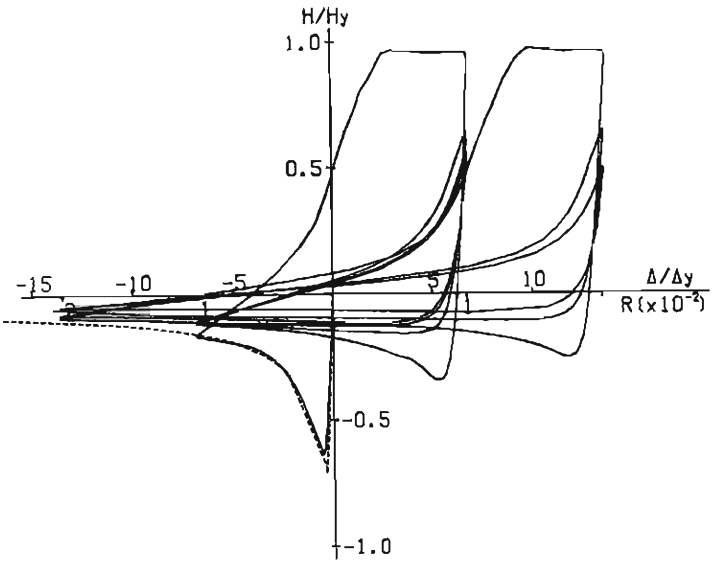

(c) SAC3

Fig. 8. H/H_y–$\Delta/_y$ Relation of Angle Braces.

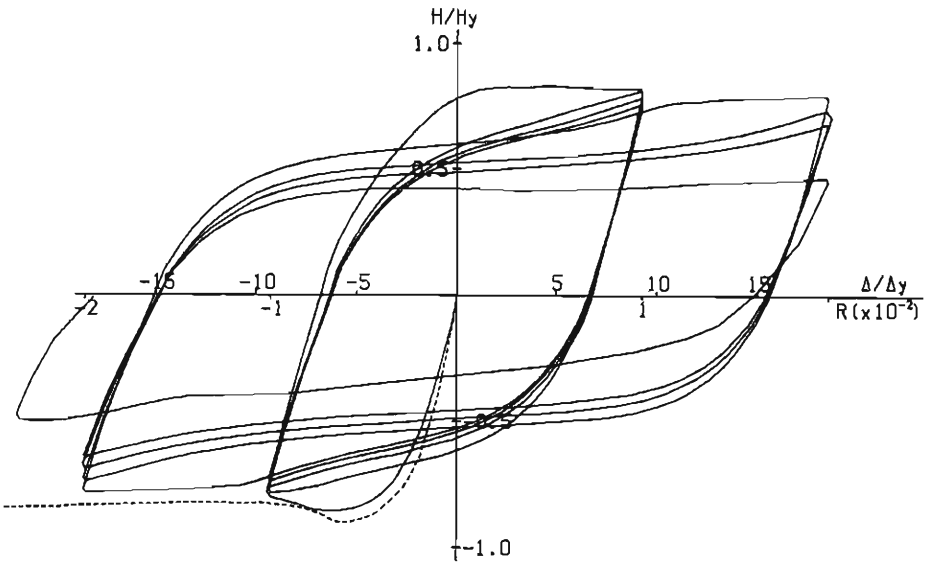

(d) DAC1

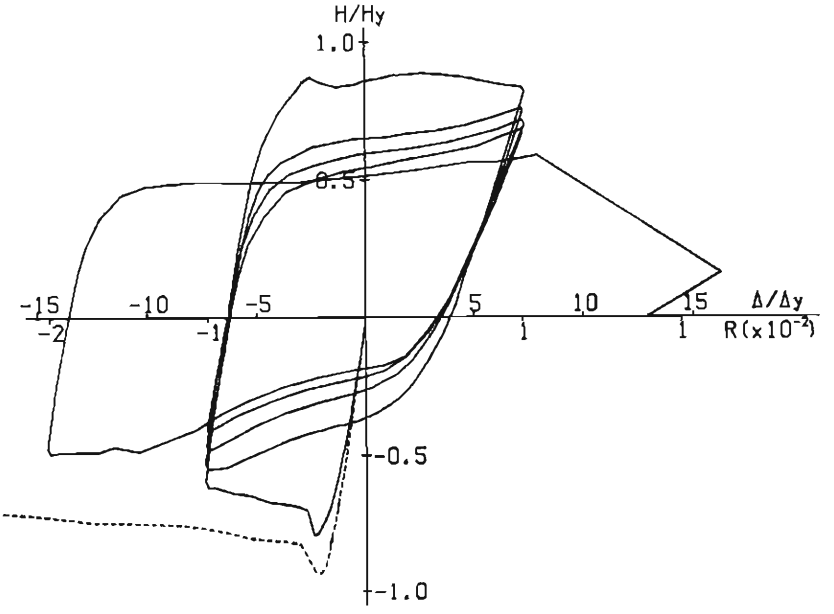

(e) DAC2

Fig. 8. H/H_y-$/\Delta_y$ Relation of Angle Braces.

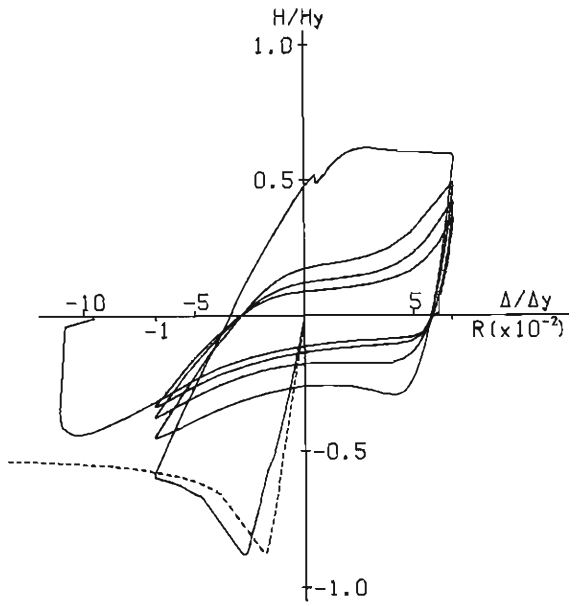

(f) DAC3

Fig. 8. H/H_y–Δ/Δ_y Relation of Angle Braces.

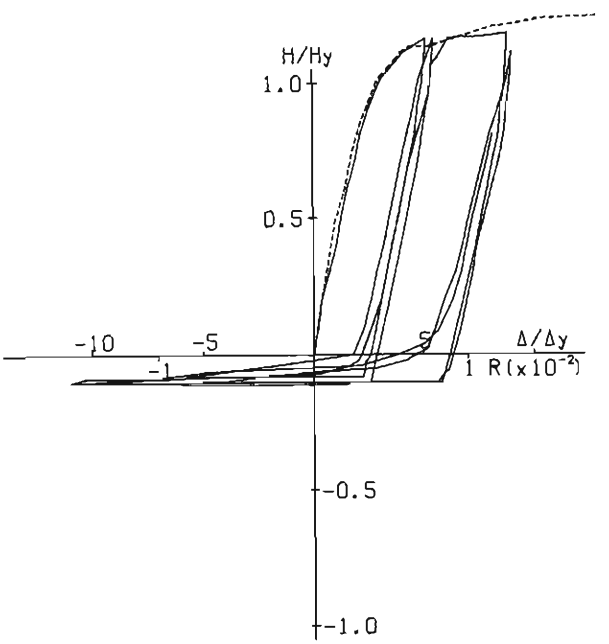

Fig. 9. H/H_y–Δ/Δ_y Relation of Flat Bar Braces.

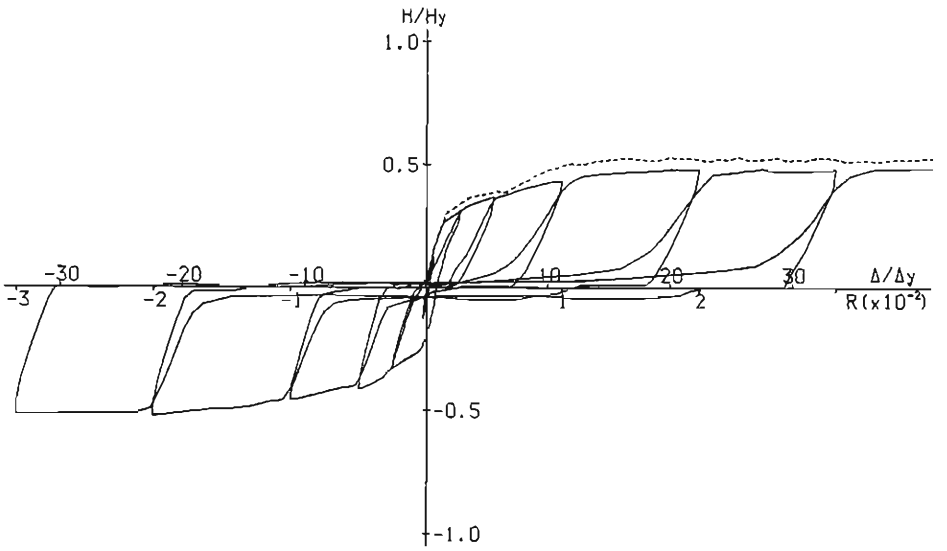

Fig. 10. H/H_y–Δ/Δ_y Relation of Round Bar Braces.

(a) DPC1 (b) DPC3

Photo. 5. Specimens after Testing.

(a) Single braces subjected to monotonic loading (SPM 1, SPM 3)

It is needless to say that the maximum load carrying capacity of braces depends upon the slenderness ratio, since horizontal load is applied in the direction that the brace should be subjected to compressive axial force. All specimens buckle in the out-of-plane of a frame. After buckling, a brace gradually changes from a circular cross sectional shape to an elliptical one at the mid-length cross section as lateral deflection increases (**Photo. 6**) and large out-of-plane bending deformation of the gusset plates takes place at the end of a brace (**Photo. 7**).

(b) Single braces subjected to cyclic loading (SPC 1, SPC 3)

Cracks take place near the welded portion at the junction between the bottom of slits in a tube and the tip of a gusset plate (**Photo. 8**) and necking in the cracked cross section takes place subsequently. The breakage of a brace is initiated in the comparatively early stage of loading. In the case of the specimen named SPC 1 ($\lambda=38$), cracks take place in tension loading in the second cycle of loading under the

Photo. 6. Deformation of Cross Sectional Shape (SPC1)

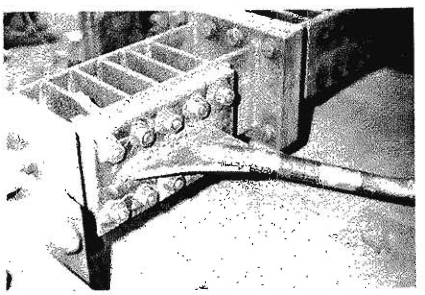

Photo. 7. Bending Deformation of Gusset Plate (SPM1)

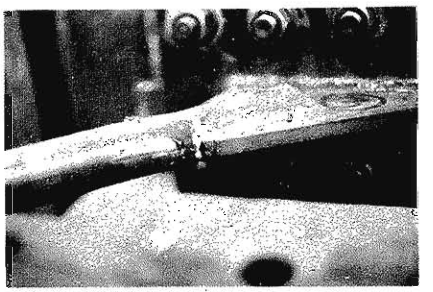

Photo. 8. Crack Initiation at the Edge of Gusset Plate.

amplitude $R=1.0\times10^{-2}$ ($\Delta/\Delta_y=7.0$). After more two cycles of loading in the same deformation amplitude, the amplitude is increased to $R=2.0\times10^{-2}$ ($\Delta/\Delta_y=14.0$) in a compression range. In the subsequent tension loading range, the breakage of a brace occurs at $R=0.75\times10^{-2}$ ($\Delta/\Delta_y=5.3$).

In the case of SPC 3 ($\lambda=109$), a crack initiation is slightly delayed to SPC 1 but the specimen is broken at $R=1.4\times10^{-2}$ ($\Delta/\Delta_y=7.9$) in a tension range of the fifth cycle of loading, just after cracks are observed.

(c) Double braces subjected to monotonic loading (DPM 1, DPM 2, DPM 3)

In the case of DPM 1 ($\lambda=36$) which is the shortest one, the brace in tension is broken at $R=1.4\times10^{-2}$ ($\Delta/\Delta_y=10$) after cracks take place at $R=1.0\times10^{-2}$ ($\Delta/\Delta_y=7.0$) near the welded portion between slits in a tube and the tip of a gusset plate. After the breakage of the tension brace, restoring force of the system gradually decreases as the deformation increases since only the compression brace is effective against horizontal load. In the cases of DPM 2 and DPM 3, a deterioration of load carrying capacity of the bracing system occurs in the range just after the buckling of a compression brace is observed. However, in the large deformation range, $R>2.0\times10^{-2}$ ($\Delta/\Delta_y=12.5$) for DPM 2 and $R>1.0\times10^{-2}$ ($\Delta/\Delta_y=5.5$) for DPM 3, the load carrying capacity of about three quaters of the maximum capacity is maintained since strain-hardening in the tension brace compensate for a decrease of load carrying capacity of the compression brace.

(d) Double braces subjected to cyclic loading (DPC 1, DPC 3)

Crack initiation and a subsequent breakage of a tension brace take place in a comparatively small deformation amplitude as well as in the case of single braces subjected to repeated loading.

The specimen named DPC 1 ($\lambda=36$) shows spindle shaped stable hysteresis loops under the deformation range $-0.5\times10^{-2}\leqq R\leqq0.5\times10^{-2}$ ($|\Delta/\Delta_y|\leqq3.5$) in which

lateral deflection due to buckling was not observed. In the third cycle of loading, cracks take place at the end of a tension brace as it approaches $R=1.0\times10^{-2}$ ($\Delta/\Delta_y=7.0$). After the load direction is reversed, cracks occur at the end of the opposite brace in tension and in the fourth cycle, the brace in tension in which cracks have taken place first is broken at the cracked portion (**Photo. 9**). DPC 3 ($\lambda=107$) shows hardening type hysteresis loops after the second cycle. Cracks take place in the fourth cycle and the breakage of a tension brace occurs at the cracked portion in the fifth cycle.

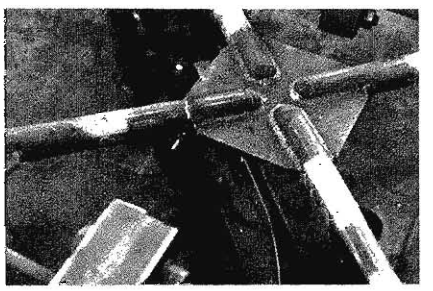

Photo. 9. Breakage of DPC1.

As above-mentioned, in the case of the circular tube brace specimen subjected to alternately repeated loading, cracks take place at the welded portion of a tube to the tip of a gusset plate in the deformation range smaller than $R=1.0\times10^{-2}$ and within about four cycles of loading. The breakage of a brace in tension occurs at the cracked portion in the small deformation range of $R=1.0\times10^{-2}$ or slightly larger value than 1.0×10^{-2} within five cycles of loading. Such small deformation capacity and the performance in less ductile manner of steel tube braces are worthy to note.

(2) Behavior of angle braces

Restoring force characteristics of angle braces obtained from experiments are shown in **Figs. 8(a)~(f)**. Peculiarities in the behavior of the braces composed of angle-shapes are represented by a large torsional deformation of an individual angle member, local buckling of leg elements and the subsequent cracking in the early stage of loading. **Photos. 10(a)** and **10(b)** show the examples of the specimens after tests.

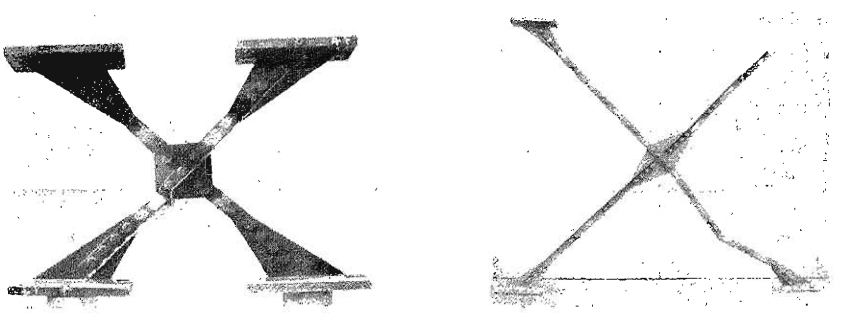

(a) DAC1 (b) DAC3

Photo. 10. Specimen after Test.

(a) Single braces subjected to monotonic loading (SAM 1, SAM 3)

In the case of SAM 1 ($\lambda=42$), torsional deformation in an angle component is observed just before the attainment of the maximum strength. Maximum load carrying capacity is slightly smaller than the yield value under pure tension. In the subsequent loading, local deformation at the buckled portion is severely predominant (**Photo. 11**).

Photo. 11. Specimen after Test (SAM1).

Maximum load carrying capacity of SAM 3 ($\lambda=106$) is attained in an ordinary flexural buckling. Local buckling of leg elements of angles takes place at the mid-length point as soon as flexural buckling occurs. In the subsequent stage of loading, local bucklings also take place near the both ends and thereafter plastic deformation is concentrated at these three locally buckled portions (**Photo. 12**).

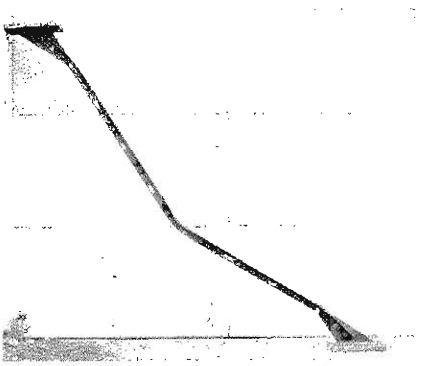

Photo. 12. Specimen after Test (SAM3).

(b) Single braces subjected to alternately repeated loading (SAC 1 and SAC 3)

In the case of SAC 1 ($\lambda=42$), behavior near the maximum load capacity is almost similar to that of SAM 1. In the third cycle of the range $-2.0\times10^{-2}\leqq R\leqq 2.0\times10^{-2}$ ($|\Delta/\Delta_y|\leqq 18.6$), the width of cracks at the locally buckled portion is rapidly enlarged and load carrying capacity is decreased severely (**Photo. 13**). Necking of a cross section with bolt holes is also observed under tension loading.

In the case of SAC 3 ($\lambda=106$), local buckling of legs of angles at the mid-length portion takes place in the first cycle of $-1.0\times10^{-2}\leqq R\leqq 1.0\times10^{-2}$ ($|\Delta/\Delta_y|\leqq 6.8$), and at the both ends in the third cycle. Plastic deformation concentrates in the locally buckled portion. In the fifth cycle, fatigue cracks take place at the mid-length portion, and in the sixth cycle, cracks take place in the tension side of a cross section in bending at the end connection and a breakage is initiated (**Photo. 14**).

(c) Double braces subjected to monotonically increasing horizontal load (DAM 1, DAM 2 and DAM 3)

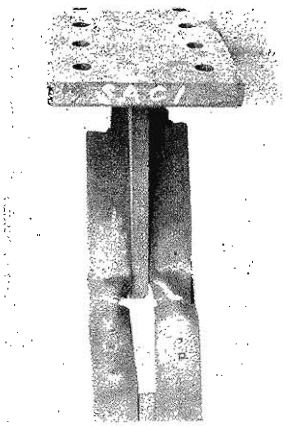

Photo. 13. Breakage due to Low Cycle Fatigue (SAC1).

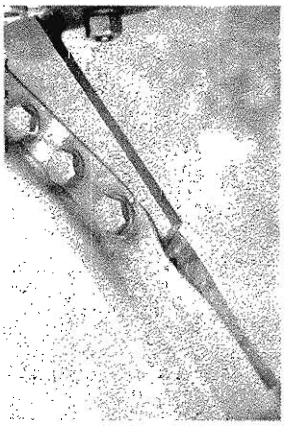

Photo. 14. Breakage of Flange at Bolt Hole (SAC3).

In the case of DAM 1 ($\lambda=34$), rigidity is gradually decreased from the beginning of loading and the maximum load carrying capacity is attained at about $R=0.5\times10^{-2}$ ($\Delta/\Delta_y=4.7$) where large torsional deformation takes place. After the maximum strength, plastic deformation concentrates in the twisted portion. In the range of $R\geqq1.0\times10^{-2}$ ($\Delta/\Delta_y\geqq9.3$), load carrying capacity is maintained in 88% of the maximum load capacity and breakage occurs at about $R=5.0\times10^{-2}$ ($\Delta/\Delta_y=50$).

In the cases of DAM 2 ($\lambda=53$) and DAM 3 ($\lambda=83$), a bottom half length of the brace in compression begins to deflect laterally nearly before the attainment of maximum load carrying capacity and subsequently local buckling takes place at the mid-length portion of the bottom half and load carrying capacity deteriorates abruptly. In the range of $R>1.0\times10^{-2}$ ($\Delta/\Delta_y\geqq7\sim9$), load carrying capacity is almost constantly maintained in about 73% of the maximum value for DAM 2 and 61% for DAM 3 by the assistance of strain-hardening in a tension brace. Necking of a cross section takes place at the end section with bolt holes when R reaches 3.0×10^{-2} ($\Delta/\Delta_y=20$) and breakage occurs soon thereafter.

(d) Double braces subjected to repeated load

Behavior of DAC 1 ($\lambda=34$) near the maximum load in the first cycle is almost similar to DAM 1. Brace elements subjected to compression buckles accompanying large torsional deformation. However, in the deformation range $-1.0\times10^{-2}\leqq R\leqq1.0\times10^{-2}$ ($|\Delta/\Delta_y|\leqq9.3$), the specimen does not show remarkable deterioration in load carrying capacity and behaves in a stable manner, having spindle shaped hysteresis loops. In the former half stage of loading range $-2.0\times10^{-2}\leqq R\leqq2.0\times10^{-2}$ ($|\Delta/\Delta_y|\leqq18.6$), stable behavior is maintained, but in the seventh cycle, fatigue cracks take place at the buckled portion of the legs of angles. In the eighth cycle, load carrying capacity deteriorates severely and the specimen is broken in tension (**Photo. 15**).

General behaviors of DAC 2 ($\lambda=53$) and DAC 3 ($\lambda=83$), are almost similar to each other although the maximum load carrying capacities are different because of the difference of slenderness ratios. The shape of hysteresis loops are hardening types which contain slip ranges in load carrying capacities. Breakages take place

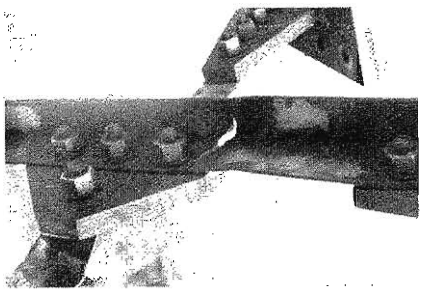

Photo. 15. Cracks due to Low Cycle Fatigue (DAC1).

in the first cycle of the loading range of $R=2.0\times10^{-2}$.

(3) Behavior of a flat bar brace

Figure 9 shows horizontal load-horizontal displacement relationships of a single flat bar braces whose slenderness ratio is about 364.

As shown clearly in the figure, load carrying capacity of a flat bar brace is very small in the compression range due to its large slenderness ratio.

Energy absorbing capacity during hysteretic loading is restricted within only one cycle in which the new plastic deformation is experienced in the tension range. Under the deformation range smaller than the once-experienced amplitude, hysteresis loops have a severely narrow shape just like a boomerang. These fundamental characteristics of the brace with a extremely large slenderness ratio are predicted theoretically using a simple analytical model.

(4) Behavior of round bar braces in which pre-tension is introduced

Figure 10 shows the experimental non-dimensionalized load (H/H_y) non-dimensionalized horizontal displacement (Δ/Δ_y) relationship of round bar braces into which pre-tension of 40% of the yield tensile force of the bar is introduced. General behavior of such pre-tensioned bar braces was described in Ref. 3) on the basis of theoretical consideration. The initial slope of the load-deflection relationship (**Fig. 10**) is nearly identical with the rigidity when two bars are effective against a horizontal load as the theory shows. However, the rigidity decreases gradually although the pre-tension in the bar under comperession is not lost yet. Disappearance of the pre-tension takes place at the horizontal load $H/H_y=2.38/H_y$ that corresponds to 60% of the yield strength under pure tension which is considerably lower than 80% of the yield strength which is predicted by the theory for the ideal model. Buckling of the brace under compression occurs at $H/H_y=2.40/H_y$, and thereafter the rigidity becomes smaller and it is considerably smaller than 1/2 of the initial value predicted by theory. Early disappearance of the pre-tension and the lower rigidity would be influenced according to the behavior of a turn-buckle. The load-displacement curve has two plateaus between buckling of a compressed brace and yielding of a brace in tension. The plateaus in the load-displacement relationship would be caused by yielding of a turn-buckle in a comparatively early stage of loading. Energy absorbing properties in the large plastic deformation range is almost same as in the case of a flat bar brace. **Photo. 16** shows the round bar brace specimen under testing.

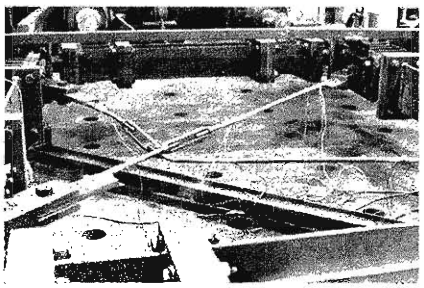

Photo. 16. Test View of Round Bar Brace.

4. Considerations on the test results

4.1 Effective slenderness ratio

Fig. 11 shows buckling stress versus effective slenderness ratio relationships obtained from the tests of circular or angle-shape braces. In the figure, marks denote the experimental results. The curves shown by EULER denotes the theoretical elastic buckling stress. The curve shown by AIJ denotes the basic column curve in the inelastic range in the AIJ Standard. Solid curve and dashed curve correspond to angle braces and circular tube braces, respectively.

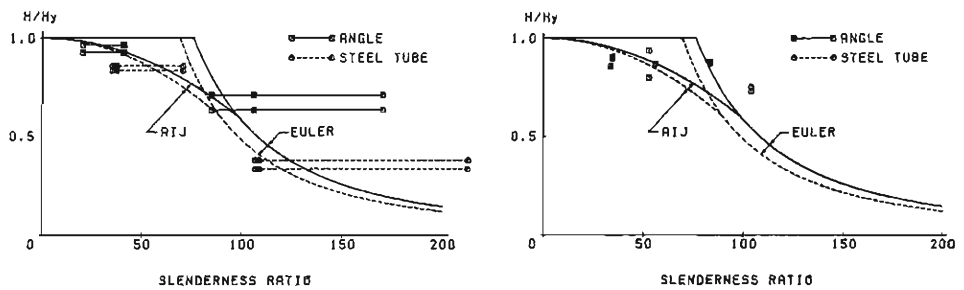

(a) Single Bracing (b) Double Bracing

Fig. 11. Buckling Stress-Slenderness Ratio Relation.

Fig. 11(a) shows the results of the single bracing case. In the case of the circular tube braces, the experimental buckling stress of a brace is plotted on the three values of calculated effective slenderness ratios. The largest slenderness ratio is calculated corresponding to the effective length for buckling which is measured as the distance between the exterior ends of gusset plates. The smallest one is a half of the largest one, that is corresponding to the rigidly fixed support conditions at the exterior ends of the gusset plates. The intermediate value between the above-mentioned two points is calculated by the theoretical analysis taking the out-of-plane bending rigidity of gusset plates into consideration. In the case of angle braces, two extreme values for the slenderness ratio for a brace are calculated using the effective length equal to the distance between the centers of gravities of bolt groups at the both ends and a half of it and the solid marks are calculated using the effective

length corresponding to a half of the distance between the intersecting points of the longitudinal axis of a brace and the longitudinal axis of the upper and the lower beams of the surrounding frame. Reasonable agreement between the experimental values and the basic column curve is observed in the use of the intermediate value of slenderness ratios.

Fig. 11(b) shows the results of the double bracing case. Experimental buckling stress is calculated from a half of the maximum load carrying capacity and plotted on the slenderness ratio shown in **Table 1**.

4.2 Load carrying capacity, energy absorbing capacity and hysteretic restoring force characteristics

The fundamental configuration of the hysteresis loops of circular tube braces and angle-shape braces are essentially similar to those of the braces with an H-shaped cross section which are reported in Part 1[1]. No peculiarity in the configuration of the hysteresis loops is observed.

Figures 12(a), **(b)** and **Figs. 13(a)**, **(b)** show the non-dimensionalized maximum load carrying capacity in each cycle versus the number of a loading cycle and the non-dimensionalized absorbed energy in a loop under repeated loading versus number of a loading cycle, respectively. The maximum load carrying capacity and the absorbed energy by a loop are non-dimensionalized by the yield horizontal load and the absorbed energy by an elastic-perfectly plastic model subjected to the identical displacement history, respectively.

The load carrying capacity and the energy absorbing capacity in the present tests have the following characteristics compared with those of the braces with an H-shaped cross section reported in Part 1[1]. **Figs. 14(a)~(d)** shows the comparison of a translation of the load carrying capacity of the specimens tested here with that of the braces with an H-shaped cross section. **Figs. 15(a)~(d)** shows the comparison

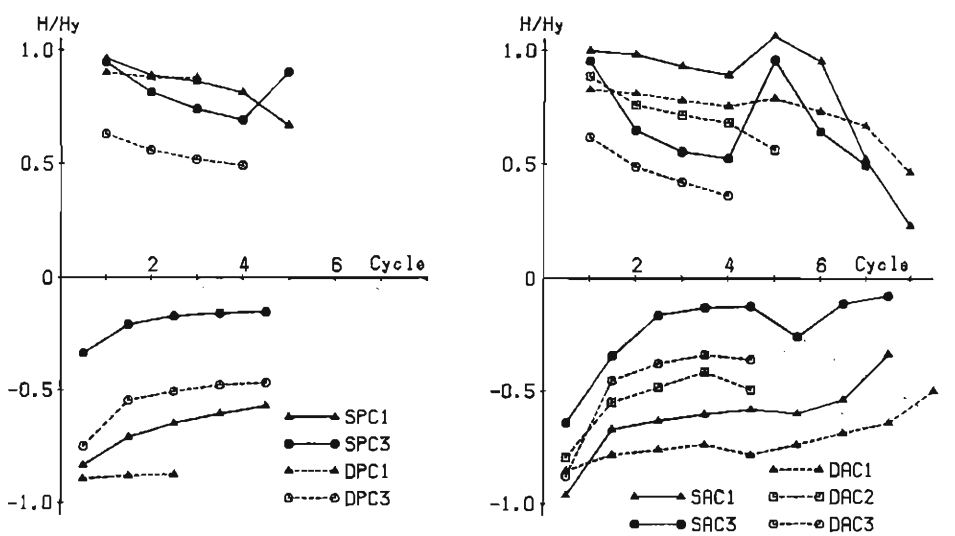

(a) Steel Tube Brace (b) Angle Brace

Fig. 12. Maximum Load Carrying Capacity in Each Cycle of Loading.

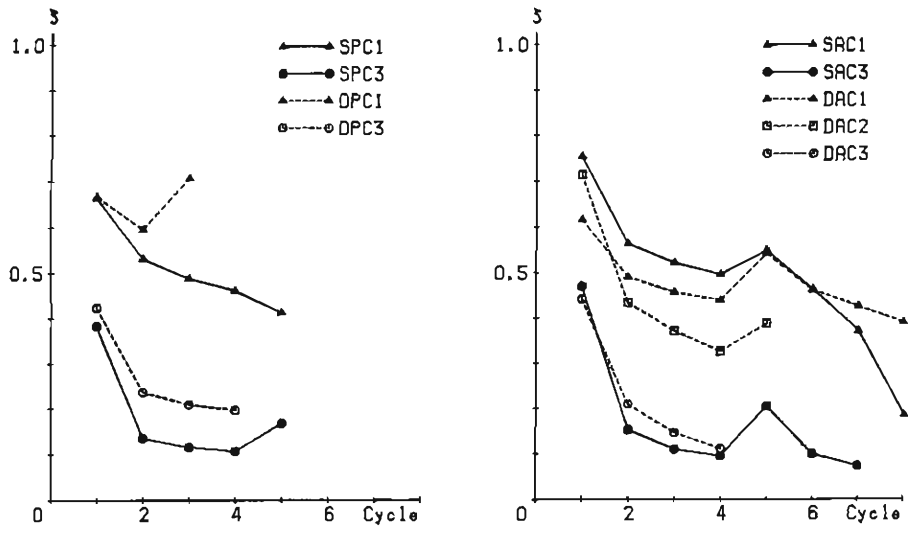

(a) Steel Tube Brace (b) Angle Brace

Fig. 13. Nondimensional Absorbing Energy in Each Cycle of Loading.

of the energy absorbing capacity. In **Figs. 14** and **15**, the numerals in the parentheses at the right side of the specimen name denote the slenderness ratio of a brace. With regard to the deterioration of the load carrying capacity with increasing a loading cycle, the deterioration of the maximum load carrying capacity in the second cycle of circular tube braces is slightly smaller than that of braces with an H-shaped cross section as shown in **Figs. 14(a)** and **14(b)**. After the second cycle, deterioration characteristics have an almost similar tendency. Remarkable differences

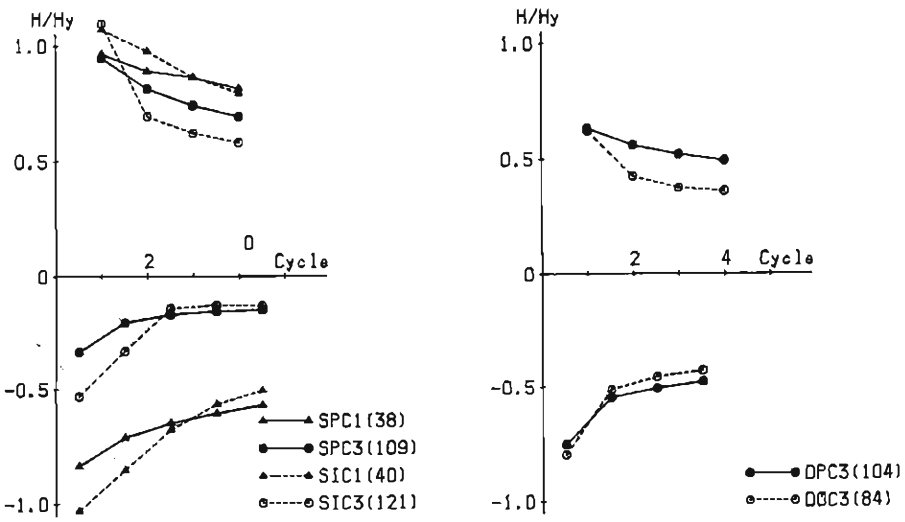

(a) Steel Tube Brace (Single Bracing) (b) Steel Tube Brace (Double Bracing)

Fig. 14. Comparison of Maximum Load Carrying Capacity.

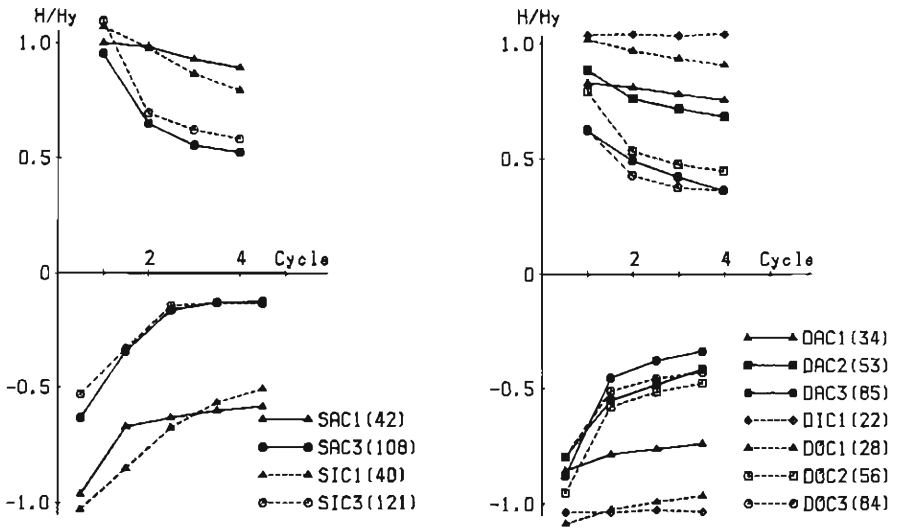

(c) Angle Brace (Single Bracing) (d) Angle Brace (Double Bracing)

Fig. 14. Comparison of Maximum Load Carrying Capacity (continued).

between the non-dimensionalized energy absorbing behaviors in the increasing loading cycle of circular tube braces and that of braces with an H-shaped cross section is not observed, as shown in **Figs. 15(a)** and **15(b)**.

In the case of angle braces, deterioration characteristics of load carrying capacity and energy absorbing characteristics are qualitatively similar to those of braces with an H-shaped cross section as shown in **Figs. 14(c)** and **14(d)**, and **Figs. 15(c)** and **15(d)**, respectively. Although, general characteristics of hysteretic horizontal

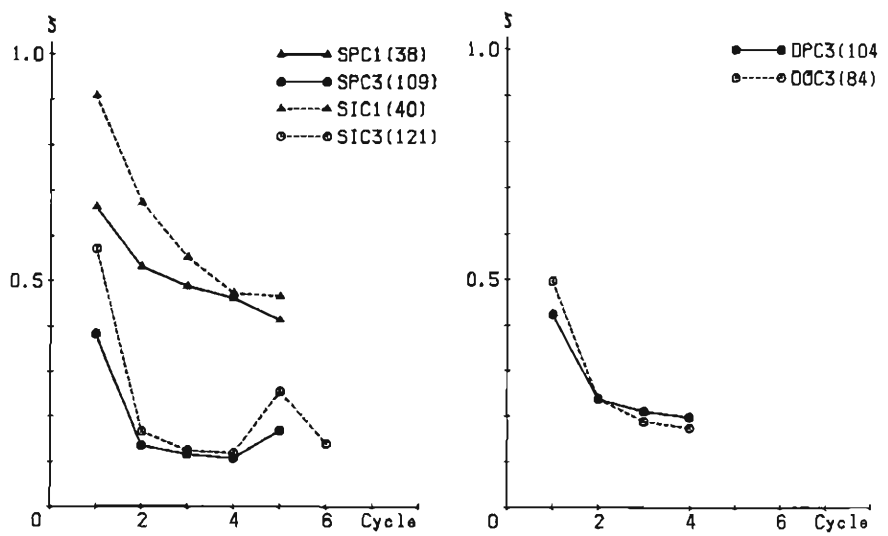

(a) Steel Tube Brace (Single Bracing) (b) Steel Tube Brace (Double Bracing)

Fig. 15. Comparison of Energy Absorption.

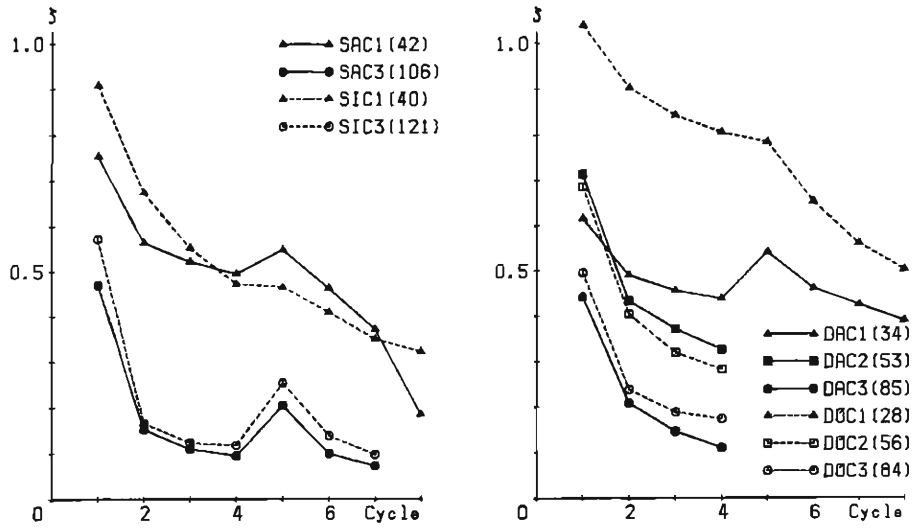

(c) Angle Brace (Single Bracing) (d) Angle Brace (Double Bracing)

Fig. 15. Comparison of Energy Absorption (continued).

load-horizontal displacement of circular tube braces and angle braces are not remarkably different from those of braces with an H-shaped cross section, considerably large difference in the deformation capacity or in the deformations when the breakage of a tension brace occurs is observed.

4.3 Characteristics of local deformation and breakage

In the case of circular tube braces, large local deformation of a cross section does not take place. In the large deformation range, it is observed that the shape of a circular cross section at the mid-length point where a transverse deflection is largest tends to become elliptical as the deflection increases. The breakage of the specimen under tension does not occur at this portion but at the end portion.

In the case of angle braces, local buckling of legs of angles is conspicuous. Local buckling is apt to take place at the external tip edge of the leg as soon as the buckling of angles takes place in the first cycle of loading. After local buckling takes place, large plastic deformation due to bending deformation of a brace concentrates at these locally buckled portions. Cracks due to low cycle fatigue under the large cyclic plastic deformation in repeated compression and tension take place at these portions and the breakage of a brace is initiated. In the specimens DAM 1 and DAC 1 which do not buckle flexurally, remarkable torsional deformation of a cross section occurs near the attainment of the maximum load carrying capacity. Thereafter this portion is obliged to be subjected to a large local plastic deformation under repeated loading. The breakage of a brace takes place at this portion after a large number of fatigue cracks take place with narrow spacings. Typical examples of the process up to the breakage is shown schematically in **Fig. 17** and **Photos. 17~18**.

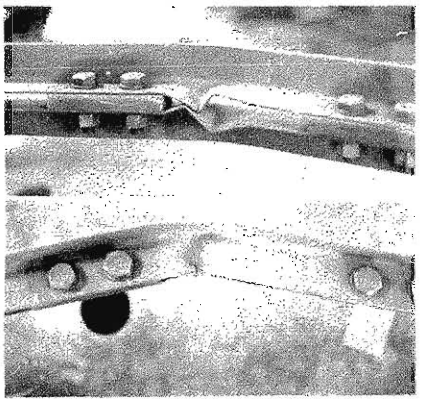

Photo. 17. Concentration of Bending Deformation at Locally Buckled Portion (DAC3).

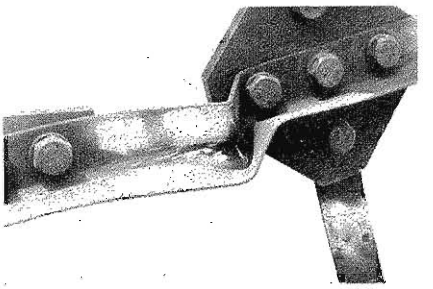

Photo. 18. Cracks with Narrow Spacings (DAC1).

4.4 Behavior near joints

(a) Circular tube braces

Near the slitted portion of the end of a steel tube subjected to a tension to which a gusset plate is fillet-welded, cracks take place in a comparatively small deformation range. As soon as cracks are initiated, crevices in cracks are expanded and necking of a cross section starts at the cracked portion. And soon, the breakage is initiated. In the case of the circular tube brace specimens, this type of failure takes place without an exception. **Fig. 16** shows the illustration of the procedure of this type of failure.

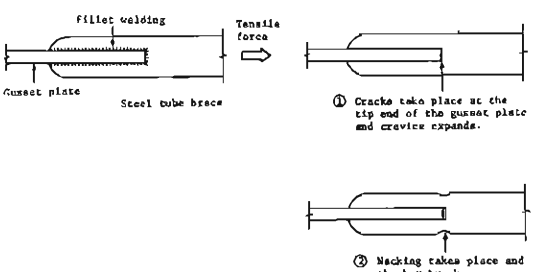

Fig. 16. Schematic Figure of Breakage of Steel Tube Braces.

(b) Angle braces

In the case of angle braces, cracking and breakage take place at the cross section with a bolt hole near the tip of a gusset plate. Two cases of crack initiation are observed. One is shown in **Fig. 17(b)**. Cracks take place in the edge of a bolt hole during a tension loading. The other is illustrated in **Fig. 17(c)**. A crack takes place in the exterior edge of a cross section with a bolt hole during compression loading. The breakage of a brace takes place in the subsequent tension loading. The number of loading in which the crack initiation and the breakage are observed

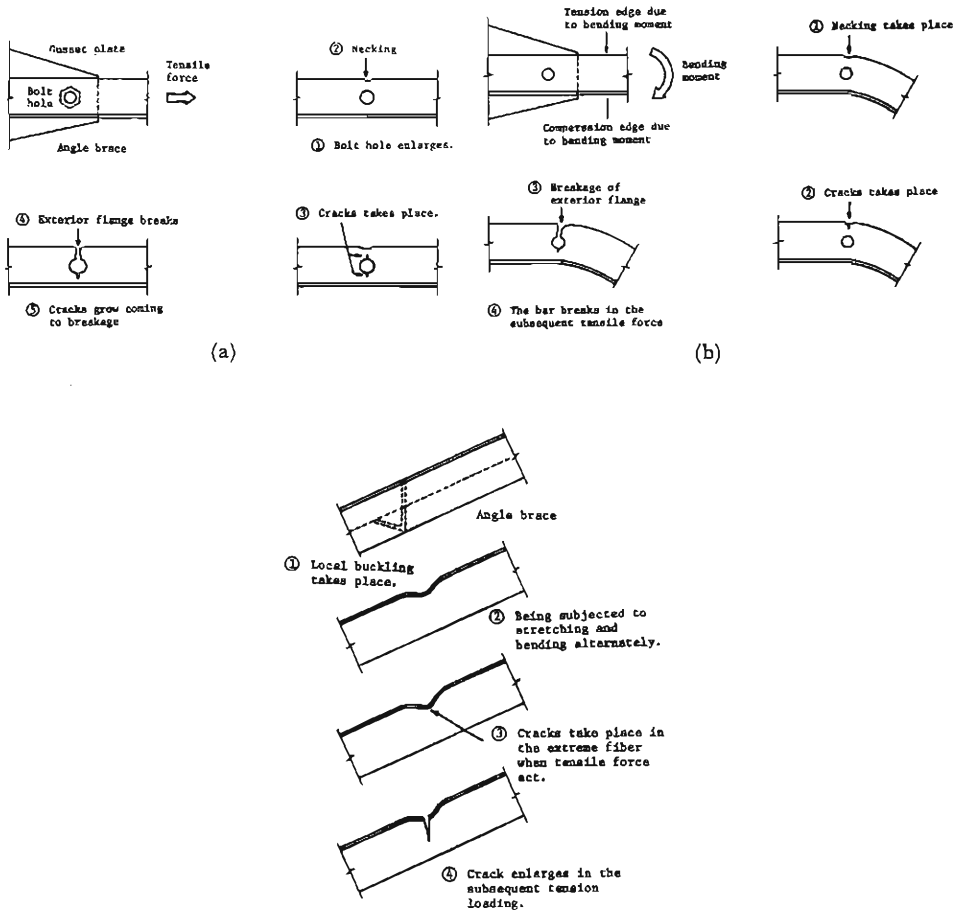

Fig. 17. Schematic Figures of Breakage of Angle Braces.

in the tests are tabulated in **Table 3** for all of the specimens. It is worthy to note that the crack initiation and the breakage are observed in a comparatively small deformation range in both cases of circular tube braces and angle braces.

Table 3. Summary of Test Result of Steel Tube and Angle Braces

Specimen Name	Local Buckling			Crack Initiation			Breakage			Other Remarks				$\frac{H_{cr}}{H_y}$
	*1 C	*2 P	R(×10⁻²)	*1 C	*2 P	R(×10⁻²)	*1 C	*2 P	R(×10⁻²)	*1 C	*2 P	R(×10⁻²)	Comment	
SPM1														0.859
SPC1				2	3	−0.10								0.835
SPM3														0.378
SPC3				5	3	1.11	5	3	1.46					0.335
DPM1								7	1.04					0.906
DPC1				3	7	−0.81	4	9	−3.88					0.893
				3	6	−0.36								
DPM2														0.868
DPM3					6	−5.58								0.721
					10	−6.04								
DPC3				2	6	0.93								0.751
				4	7	−0.86								
SAM1		2	−0.18											0.926
SAC1	1	1	0.28	7	1	−0.43								0.964
SAM3		2	−1.25											0.709
SAC3	1	2	−0.08	3	2	1.01				7	3	2.02	Necking at Bolt Hole	0.634
				7	3	−2.02								
DAM1		1	−0.43								7	−3.42	Necking at Bolt Hole	0.854
		5	−3.20											
DAC1	1	3	−0.56	6	2	2.02								0.856
	1	9	−0.16	7	10	−1.31								
DAM2		5	−0.49		10	−3.29					10	−3.50	Necking at Bolt Hole	0.936
		4	−0.59											
DAC2	1	5	−0.33	5	11	−1.59	5	5	2.25					0.797
	1	11	−0.28	5	5	1.10								
DAM3		2	−0.30		9	−3.39					9	−3.29	Necking at Bolt Hole	0.811
DAC3	1	3	−0.96	1	10	0.38	5	6	−1.61	2	6	−1.02	External	0.876
	2	4	−0.29	3	5	0.46				3	5	0.54	Part of Leg with a Bolt Hole Breaks.	
	2	5	−0.29											
	2	11	0.91											

*1: Number of Cycle

*2: Number of Position

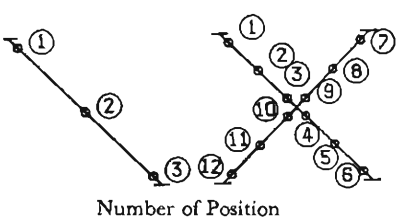

Number of Position

5. Concluding Remarks

From the experimental investigation on the hysteretic behavior and the behavior upto the breakage of steel braces under repeated horizontal loading, whose cross sectional shapes and design details at the end joints are frequently applied to the actual design of steel framed structures, the following remarks can be drawn.

(i) There is no significant difference between general characteristics of hysteresis loops of angle braces and those of the braces with an H-shaped cross section, although the local buckling or torsional deformation take place in angle braces.

(ii) Deterioration of the load carrying capacity and energy absorbing capacity in the second cycle of loading of circular tube braces are slightly smaller than those of braces with an H-shaped cross section, but general characteristics of hysteresis loops are quite similar.

(iii) Although no significant difference in the shape of hysteresis loops due to the difference in cross sectional shapes of braces are observed, the difference in the plastic deformation capacity under repeated loading is considerably large. Cracking near the welded portion between the tip of the gusset plate and the bottom of slits of a circular tube brace section and cracking at the end section with bolt holes of angle braces causes the breakage of braces in the comparatively early stage of loading. Cracks in the circular tube brace take place at the portions where stress concentration exists. Therefore, sufficient consideration for design of details in connections and complete fabrication are called for. Cracks at the end section with bolt holes and cracks in the mid-section where local buckling occurs could be caused by low cycle fatigue of the plate elements of angles under repetition of large plastic deformation in cyclic loading. Appropriate reinforcement in such sections may be expected to maintain the ductility of the members. Detailed investigation on local failure and reinforcing methods are remained in the future.

(iv) With regard to the restoring force characteristics of braces with extremely large slenderness ratio such as flat bar braces and round bar braces, load carrying capacity under compression is not expected and energy absorbing capacity due to repeated loading is not anticipated except the first chance in which the brace experiences a new plastic deformation in the yield plateau in tension, as reasonably as the theoretical approach predicts.

(v) In the case of the pre-tensioned round bar braces, the behavior of turn-buckles is apt to characterize the hysteretic behavior of braces. Details of the behavior of turn-buckles should be investigated.

Acknowledgement

This investigation was supported by the Building Research Institute, Ministry of Construction.

The authors wish to present their gratitudes for Mr. Hironi Masuda, the former graduate student of Osaka Institute of Technology and Messrs Masahiko Taniguchi and Hidezo Hashimoto, the former students of Osaka Institute of Technology who greatly assisted the laborious experimental work.

References

1) Wakabayashi, M., T. Nakamura and N. Yoshida: Experimental Studies on the Elastic-Plastic Behavior of Braced Frames under Repeated Horizontal Loading, Part 1, Experiments of Braces with an H-shaped Cross Section in a Frame, Bull. Disast. Prev. Res. Inst., Kyoto University, Vol. 27, Part 3, No. 251, Sept. 1977, pp. 121–154.

2) Wakabayashi, M., T. Nakamura, A. Katagihara, H. Yokoyama and T. Morizono: Experimental Studies on Elastic-Plastic Hysteretic Behavior of Flat Bar Braces Cased in Concrete Wall without Bound, Part 1, Preliminary Tests, Proc. of Annual Convention of Kinki Section of AIJ, June 1973, pp. 121–124.

3) Wakabayashi, M.: The Behavior of Steel Frames with Diagonal Bracings under repeated Loading, Proc. of Japan-U.S. Seminar on Earthquake Engineering with Emphasis on the Safety of School Buildings, Sendai, Japan, 1970, pp. 328–345.

Notations

B : Diameter or width
C : Number of cycles of loading
H : Horizontal load
H_{cr} : Horizontal load at first buckling
H_y : Yield horizontal load
l : Distance between the exterior ends of gusset plates, or between the pins in the case of round bar braces
l' : Distance between the interior ends of gusset plate in the case of steel tube and round bar braces or between the centers of gravity of bolt groups in the case of angle braces
P : Number showing the postition of the bar
R : Ratio of Δ to the clear height of column, or rotation angle of column
t : Thickness
Δ : Story drift
Δ_y : Yield horizontal displacement
λ : Effective slenderness ratio
λ_1 : Slenderness ratio using the length $l/2$ (steel tube) or $l'/2$ (angle)
λ_2 : Twice λ_1
λ_3 : Slenderness ratio taking into account of the bending rigidity of gusset plate (steel tube), or taking a half distance of the intersections of longitudinal axes of two beams and braces
ζ : Nondimensional absorbed energy